iScience

CellPress
OPEN ACCESS

Article

A method for rapid nanobody screening with no bias of the library diversity

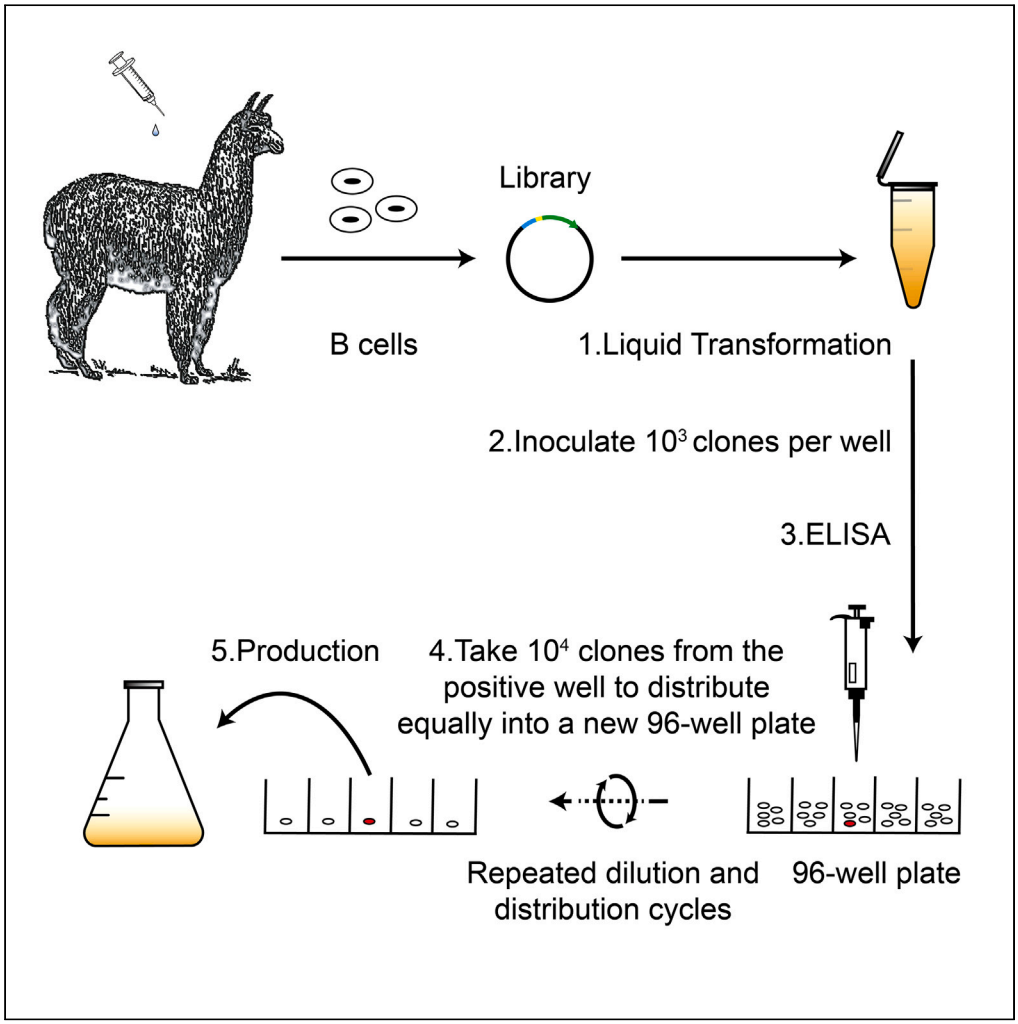

Zhiqing Tao, Xiaoling Zhao, Huan Wang, ..., Xu Zhang, Maili Liu, Lichun He

helichun@apm.ac.cn

Highlights

Screening of nanobodies without any specialized instruments

Isolation of nanobodies with a broad range of binding affinities

Integrated way of screening and expression of nanobodies

Tao et al., iScience 27, 108966
February 16, 2024
https://doi.org/10.1016/j.isci.2024.108966

iScience

CellPress
OPEN ACCESS

Article

A method for rapid nanobody screening with no bias of the library diversity

Zhiqing Tao,[1,2,8] Xiaoling Zhao,[3,4,8] Huan Wang,[5,8] Juan Zhang,[3] Guosheng Jiang,[5] Bin Yu,[1,2] Yihao Chen,[1,2] Mingjun Zhu,[1,2] Junli Long,[1,2] Lei Yin,[6] Xu Zhang,[1,2] Maili Liu,[1,2,7] and Lichun He[1,2,9,*]

SUMMARY

Nanobody, referred to the variable domain of heavy-chain-only antibodies, has several advantages such as small size and feasible *Escherichia coli* expression, making them promising for scientific research and therapies. Conventional nanobody screening and expression methods often suffer from the need for subcloning into expression vectors and amplification-induced diversity loss. Here, we developed an integrated method for simultaneous screening and expression. Nanobody libraries were cloned and secretly expressed in the culture medium. Target-specific nanobodies were isolated through 1–3 rounds of dilution and regrowth following the Poisson distribution. This ensured no dismissal of positive clones, with populations of positive clones increasing over 10-fold in each dilution round. Ultimately, we isolated 5 nanobodies against death domain receptor 5 and 5 against Pyrococcus furiosus DNA polymerase directly from their immunized libraries. Notably, our approach enables nanobody screening without specialized instruments, demonstrating broad applicability in routine monoclonal nanobody production for diverse biomedical applications.

INTRODUCTION

Single-domain antibody also named nanobody, refers to the variable domain from the heavy-chain-only antibody (VHH).[1] Nanobody emerges as an alternative to the traditional antibody as it has several unique properties, such as high solubility, excellent stability, and small size (10–15 kDa).[2] Unlike the normal monoclonal antibody, nanobody can be expressed in *E. coli* with a high yield. Fusing the N terminus of a nanobody with a secretion signal peptide can lead to the secretion of the nanobody into the periplasmic space and the extracellular milieu through the type II secretion system[3] or some other unspecific release ways.[4] Moreover, nanobodies could specifically bind the antigen with an affinity in the nanomolar range.[5] The lack of light chains facilitates nanobodies for the construction of bispecific antibodies as well as conjugations with E3 ubiquitin ligases for specific degradation of target proteins.[6] Owing to these properties of the nanobody, diverse biomedical and scientific applications of nanobody also include the usage of nanobody in hot start polymerase chain reactions (PCRs) and chimeric antigen receptor T cell (CAR-T) therapies.[7,8] Nevertheless, the isolation of nanobodies mainly follows methods used for screening traditional antibodies such as phage display, cell surface display, and ribosome display.[9] These display methods are usually labor intensive, involving separated screening and producing vector systems. The isolation of target-specific monoclonal antibodies usually takes months. Furthermore, the commonly used phage display method has been reported to suffer from the loss of library diversity during the amplification procedure.[10,11] The amplification of the screening libraries, which is a critical step for phage display, diminishes the diversity of libraries and reduces the number of different clones binding with the antigen specifically, hindering the identification of antibodies with different binding epitopes and affinities. One of the reasons is the competition of the binding between antibodies and the target molecule, which reduces the monoclonal antibodies with lower affinities. Other factors rather than the binding affinity also contribute to the loss of diversities of the library. Different peptides are presented unequally by phages.[12] Moreover, a single phage particle infects bacteria and then secrets more than 1,000 copies of phage, which greatly enriches phages with growth advantage during any of the amplification procedures.[10] By contrast, several recent studies highlighted the importance of the diversity of antibodies. Low- or moderate-affinity rather than high-affinity antibodies deliver greater activity, even when

[1]State Key Laboratory of Magnetic Resonance and Atomic Molecular Physics, National Center for Magnetic Resonance in Wuhan, Innovation Academy for Precision Measurement Science and Technology, Chinese Academy of Sciences, Wuhan 430071, China
[2]University of Chinese Academy of Sciences, Beijing 100049, China
[3]Department of Reproductive Medicine, General Hospital of Central Theater Command of the People's Liberation Army, Wuhan, Hubei 430061, China
[4]Qinhe Life Science Ltd, Wuhan 430000, China
[5]School of Life Science and Technology, Weifang Medical University, Weifang, Shandong 261053, China
[6]State Key Laboratory of Virology, Hubei Key Laboratory of Cell Homeostasis, College of Life Sciences, Department of Clinical Oncology, Renmin Hospital of Wuhan University, Wuhan University, Wuhan, Hubei Province 430072, China
[7]Optics Valley Laboratory, Hubei 430074, China
[8]These authors contributed equally
[9]Lead contact
*Correspondence: helichun@apm.ac.cn
https://doi.org/10.1016/j.isci.2024.108966

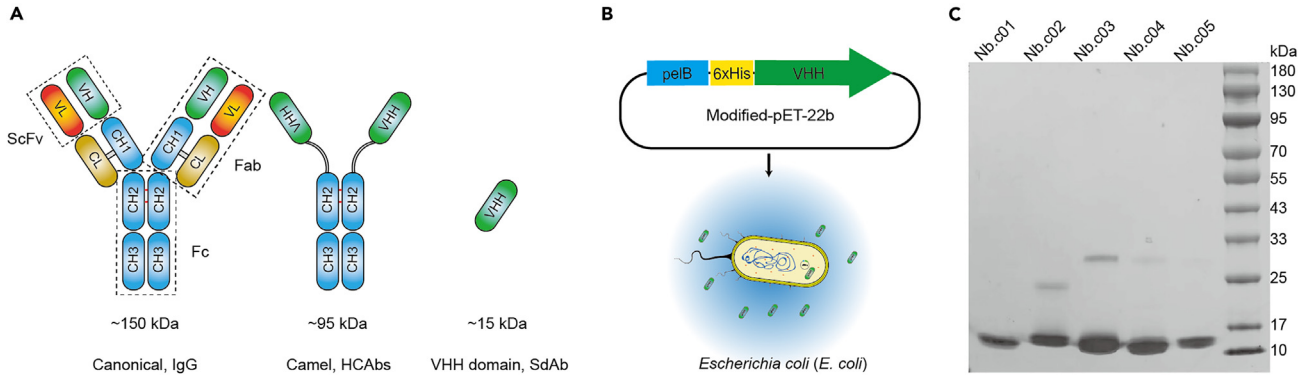

Figure 1. Unique features of nanobodies compared to conventional antibodies

(A) Schematic structures of the conventional antibody, the heavy-chain-only antibody from camel serum, and the variable fragment of heavy-chain antibodies (VHH) also named as nanobody or single-domain antibody (SdAb).

(B) Construction and modification of the pET-22b vector for expression and secretion of nanobodies by *E. coli*.

(C) SDS-PAGE analysis of various nanobodies secreted into the *E. coli* culture medium. 10 times concentrated supernatant of the cell culture medium was applied for SDS-PAGE analysis.

they share overlapping binding epitopes with the high-affinity antibody.[13–15,16] Thus, the development of new methods for antibody discoveries is needed to overcome the problem of the convergence of the library.

Here, we presented a rapid and no-biased approach to generate monoclonal nanobodies against selected targets. Two immunized libraries against the Death receptor 5 (DR5) and the Pyrococcus furiosus (*Pfu*) DNA polymerase were secretively expressed into the culture medium. With the dilution and regrowth of *E. coli* transformed with each immunized library, populations of positive nanobody clones were enriched more than 10-fold per round with no loss of the library diversity based on the mathematical calculation. The target-specific monoclonal nanobodies were then isolated and purified directly from the culture medium. Moreover, this integrated way of screening and expression of nanobodies works even without any specialized instruments, providing a robust, low-cost, and no-biased approach to generating monoclonal nanobodies against selected targets.

RESULTS

Secretion of nanobodies into the culture medium

E. coli has been used as one of the most suitable hosts for the production of recombinant proteins, such as nanobodies and antibody fragments. However, nanobodies expressed in the cytosol of *E. coli* face several problems including the formation of insoluble inclusion bodies, and the inability to form disulfide bonds correctly.[17] Both will ultimately lead to toxicity to the host cell.[18] As data from our lab showed several proteins could be secreted into the culture medium by fusing it with the pelB signal peptide (Figure S1 HdeA, Spy, Im7 secretion), we are wondering if nanobodies could be secreted into the culture medium to avoid the aforementioned toxic problems. For this purpose, we constructed expression vectors by fusing the pelB signal peptide and 6× His-tags on the N terminus of nanobodies from a commercial naive library (Qinhe Life Science Ltd.) (Figure 1B). As we expected, the preliminary experiments revealed all 5 randomly chosen nanobodies were secreted into the culture medium with a clear band on the SDS-PAGE gel (Figure 1C), proving the feasibility of secretion expression of nanobodies by *E. coli*. The secretion of nanobody into the culture medium not only enables us to screen the monoclonal nanobody in a similar way as the hybridoma technology but also allows us to integrate the screening and purification of nanobodies by using the same expression vector and host cells, which will greatly reduce the time needed for the discovery of specific binding nanobodies.

New strategy for direct isolation of specific nanobodies with simple dilution and regrown cycles

The numbers of antigen-specific immunoglobulin G (IgG)-secreting B cells in the peripheral blood range from the order of 10^{1-4} per 10^6 cells after a single immunization.[19–22] Thus, directly following the hybridoma technology by diluting an immunized nanobody library expressing *E. coli* into single cell per well to perform screening for specific monoclonal nanobodies faces the problem of low throughput.[23] To solve this problem, we designed a new strategy to mix 10^n clones per well. In this way, a single 96-well plate could reach a screening throughput of 10^{n+2}. For the convenience of calculation, 96 wells were approximated as 100 wells here and in the following text. Once the well with positive clones was identified, a division of m clones was taken out, diluted, and re-distributed equally into a new 96-well plate for the next round of isolating the specific monoclonal nanobody. Since the mixture of *E. coli* clones in each well could be considered as complete homogenous materials, the number of positive clones in the division (m) taken out from the positive well follows the Poisson distribution (Equation 1),

$$P(X) = \frac{\lambda^x}{x!}e^{-\lambda}, \lambda = m * 10^{-n} \quad \text{(Equation 1)}$$

where P(X) was the probability of taking X positive clones; λ specified the expected value of the number of positive clones in the division (m), which equaled the product of the number of clones in the division (m) and the probability of taking one positive clone (10^{-n}); and e ≈ 2.718 was the base of the natural logarithm. The probability of at least one positive clone being presented in the division (m) for diluting, distributing, and regrowing for the next round of screening could be calculated with Equation 2.

$$P(x \geq 1) = 1 - P(x \leq 0) = 1 - \sum_{i=0}^{0} P(x = i) = 1 - \sum_{i=0}^{0} \frac{\lambda^0}{0!} e^{-\lambda} \quad \text{(Equation 2)}$$

The population of positive clones will be enriched by a factor of $\frac{100}{\lambda}$ over each round of isolation. Accordingly, the probability of at least one positive clone being taken in the division (m) from the identified positive well was 0.993262, 0.999955, and 0.999999, when λ equaled 5, 10, and 20 respectively. The population of positive clones will be enriched by a factor of 20, 10, and 5 in the next round of isolation (Figure S2). A higher value of λ helped to avoid the dismission of positive clones in the process of screening. However, considering the enriching factor of positive clones over each round of screening, a λ value of 10 was used in the following study.

Assessing the performance of the new strategy with two immunized libraries

To assess the performance of the aforementioned new strategy, we first immunized two alpacas with purified antigen proteins DR5 and *Pfu* DNA polymerase. IgG titers assayed by ELISA confirmed the generation of specific camel antibodies against both antigen proteins in the serum of immunized animals (Figure S3). Total mRNA was extracted from lymphocytes according to the protocol of the LeukoLOCK Total RNA Isolation Kit. The VHH gene segments from two immunized cDNA libraries were amplified by nested PCR and then cloned into our modified pET-22b secretion vector. For *Pfu* DNA polymerase nanobodies, upon the transformation of *E. coli* with constructed nanobody-encoding vectors, the first round of screening was performed with about 10^3 clones inoculated in 2 mL terrific broth (TB) culture medium in each well of a 96 deep-well plate (A_1 plate). All wells in the A_1 plate were induced with 0.5 mM isopropyl-β-D-thiogalactoside (IPTG) for 12 h and centrifuged to collect supernatants for ELISA assay to identify the well(s) with positive clones. Since all secreted nanobodies had His-tags constructed on the N terminus, the ELISA plate was then incubated with an anti-His-tag mouse monoclonal antibody and a secondary anti-mouse antibody conjugated horseradish peroxidase (HRP) to detect specific bound nanobodies. The screening results are shown in Figures 3A–3D. Several wells showed optical density 450 (OD_{450}) values larger than 1.0, indicating *E. coli* clones expressing specific nanobodies against the *Pfu* DNA polymerase were presented in these wells. The probability of certain positive clones (p_i) was ~1‰. Cells in the positive well of the A_1 plate were then resuspended to determine the cell number by using the standard curve of the cell number and the value of OD_{600} (Figure S4). A division of ~10^4 clones was taken out from the positive well to dilute and aliquot equally into a new 96 deep-well plate (A_2) for regrowing. The expected value (λ) of the number of a certain positive clone presenting in the division was 10 according to Equation 1. The probability of positive clones taken into the division from the identified positive well was 99.995% according to Equation 2. Therefore, hardly any positive clone would be dismissed with our new strategy. As these ~10^4 clones taken from the positive well were aliquoted evenly into the A_2 plate, each well would have ~100 clones. The probability of a certain positive clone presenting in one well increased from 1‰ to 1% (Figure 2). With 2 rounds of screening, the number of clones in each well was ~10 (Figure 3C). A simple diluting and spreading of cells from the positive well on the LB agar plate with ampicillin were performed to get single-cell clones of *E. coli*. The single-cell clones were then inoculated into another 96 deep-well plate (A_3) for the final round of screening to get the specific monoclonal nanobodies (Figures 2 and 3D). In the end, 6 nanobodies against *Pfu* DNA polymerase were isolated, of which 5 different nanobodies were identified according to the calculated genetic distance[24] (Figure 3H). For DR5 nanobodies, the first round of screening with 10^2 clones inoculated per well showed all positive signals, indicating the population of DR5-specific IgG-secreting B cells was large. We then tried to isolate the DR5-specific monoclonal nanobody by picking single-cell clones from the luria broth (LB) plate to inoculate in the 96 deep-well plate with one clone per well. 22 out of 96 clones revealed positive signals from the ELISA assay, showing the high immunogenicity of DR5 (Figure 3E). 10 clones from the positive wells were picked and sent for sequencing. 5 different nanobodies were identified according to the calculated genetic distance[24] (Figure 3G). Nevertheless, we would like to point out that more different nanobodies against both *Pfu* DNA polymerase and DR5 could be isolated if needed. Both isolated *Pfu* DNA polymerase- and DR5-specific nanobody-expressing *E. coli* strains were used directly for the production of monoclonal nanobodies. After one step of purification by the nickel nitrilotriacetic acid (Ni-NTA) column, the purity of nanobodies reached >95% by SDS-PAGE (Figure S5). This integrated screening and purification of target-specific monoclonal nanobodies did not need to graft the gene of interest into a new expression vector, simplifying the discovery of nanobodies.

High throughput of the new strategy for isolating nanobodies

The screening throughput of our strategy was dependent on the number of clones inoculated per well. The signal of positive clones was highly related to its secretion level in the culture medium. For the nanobodies against *Pfu* DNA polymerase, we inoculated 10^3 clones per well, showing a screening throughput of 10^5 for a single plate. However, nanobodies against DR5 were isolated with the inoculation of a single clone per well. To demonstrate the screening throughput for DR5 nanobodies, we diluted the supernatant of each of five isolated DR5-specific nanobodies with the supernatant from *E. coli* transformed with a naive library of nanobodies by ratios of $1:10^1$, $1:10^2$, $1:10^3$, and $1:10^4$. All five nanobodies showed clear positive signals at the dilution ratio of $1:10^3$. Two DR5-specific nanobodies even showed a positive signal upon dilution by the ratio of $1:10^4$, demonstrating secretion levels of naturally occurred nanobodies in our system were fairly high to support a screening throughput of 10^5–10^6 for a single 96-well plate (Figure 3F).

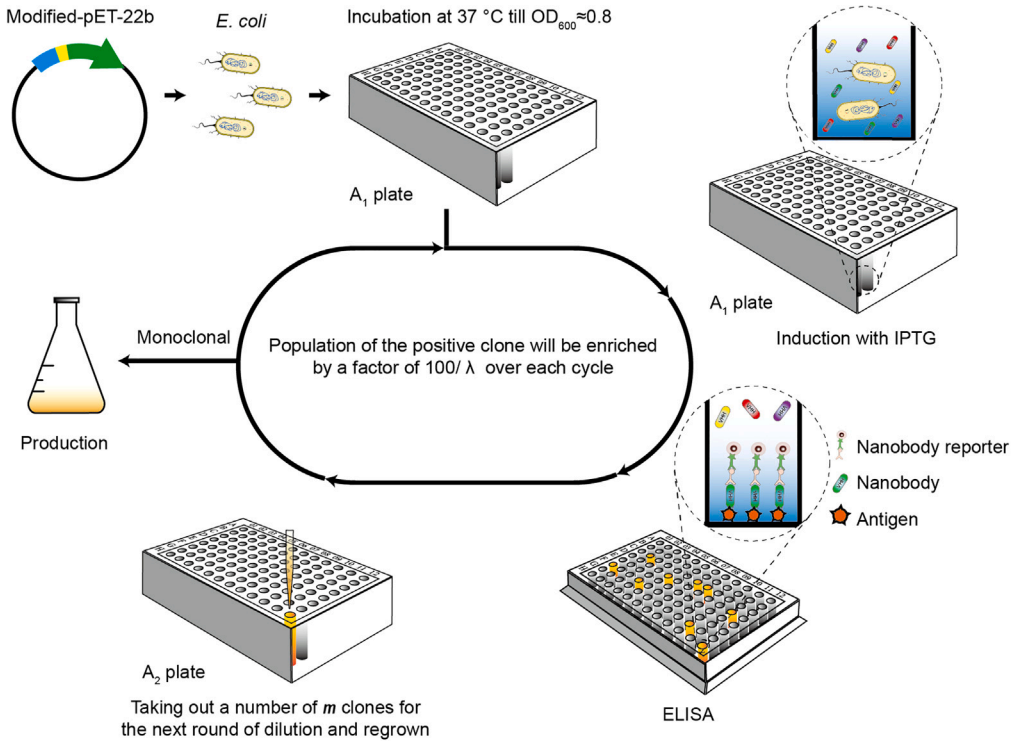

Figure 2. Scheme of integrated isolation and expression of the specific binding monoclonal nanobody via repeated dilution, distribution, and regrown cycles following the rule of Poisson distribution to avoid the dismission of the positive clones while enriching the population of positive clones

A broad range of binding affinities of isolated nanobodies against target proteins

We performed isothermal titration calorimetry (ITC) assays to access the binding affinities of isolated nanobodies. DR5, *Pfu* DNA polymerase, and their corresponding isolated nanobodies were purified and dialyzed in the same buffer 20 mM HEPES, 150 mM NaCl, pH 8.0, at 4°C overnight. The results showed binding affinities of five isolated DR5 nanobodies with DR5 ranged from 18 μM to 54 pM and the binding affinities of four isolated *Pfu* nanobodies with *Pfu* DNA polymerase ranged from 33 μM to 35 pM (Table 1; Figures 4 and S6), confirming our developed strategy had no bias with high-affinity antibodies and could be applied for isolating nanobodies with a broad range of binding affinities with target proteins.

Binding epitopes of isolated nanobodies on *Pfu* DNA polymerase

To demonstrate the diversities of isolated nanobodies, we further probed if the binding epitopes of different nanobodies on *Pfu* DNA polymerase overlapped with each other via nuclear magnetic resonance (NMR) spectroscopy. For each of the isolated *Pfu* nanobodies, both ^{15}N-labeled and unlabeled samples were expressed and purified. The ^{15}N-^{1}H heteronuclear single quantum coherence (HSQC) spectrum of each isolated nanobody was first measured in the presence and absence of *Pfu* DNA polymerase. Upon adding *Pfu* DNA polymerase, the formation of the nanobody and *Pfu* DNA polymerase complex caused a shorter T2 relaxation time and the consequent peak intensity reduction of the labeled nanobody in the spectrum (Figures 5A and S7). Then ^{15}N-^{1}H HSQC spectra of each *Pfu* nanobody were recorded in the presence of *Pfu* DNA polymerase and another different unlabeled nanobody. If two nanobodies shared overlapping binding sites on *Pfu* DNA polymerase, the addition of a second competitive unlabeled nanobody would release the ^{15}N-labeled nanobody from *Pfu* DNA polymerase and restore the peaking intensity of the ^{15}N-labeled nanobody. If two nanobodies had separated binding sites on *Pfu* DNA polymerase, the addition of a second non-competitive unlabeled nanobody would have little effect on the peaking intensity of the ^{15}N-labeled nanobody. In this way, the overall competitive status of all five nanobodies in binding with *Pfu* DNA polymerase was measured and summarized in Figure 5C. To connect the binding epitopes of the nanobody with the functional site of *Pfu* DNA polymerase, the inhibition of DNA polymerase activity of *Pfu* DNA polymerase by different nanobodies was accessed. (Figures 5D and S8). Single-stranded DNA incubation assay was performed in the presence of each individual *Pfu* nanobody and the synergetic binding reagent (SYBR) green I dye, which was used as an indicator of the final amount of double-strand DNA. The results showed the addition of either Nb.Pf02 or Nb.Pf04 strongly inhibited the polymerase activity of *Pfu* DNA polymerase, indicating that Nb.Pf02 and Nb.Pf04 bind to active sites of the polymerase domain of *Pfu* (Figure 5D). According to the mutual competitive relationship, the cartoon representation of binding sites of all five *Pfu* nanobodies was plotted in Figure 5B, with the binding site of Nb.Pf02 on the *Pfu* DNA polymerase as the reference.

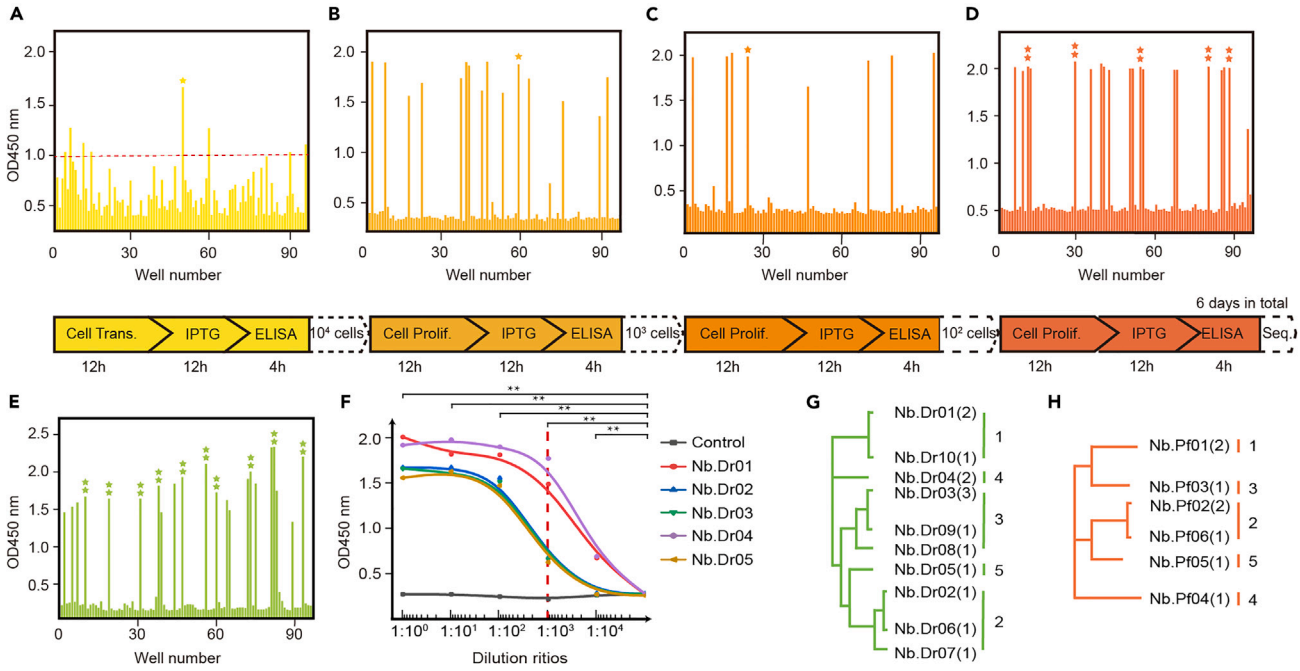

Figure 3. Isolation of nanobodies against *Pfu* DNA polymerase and DR5

ELISA results of supernatants of nanobody culture media.

(A–C) Supernatants of ~1,000 (A), ~100 (B), ~10 (C) different nanobody-expressing clones were monitored against *Pfu* DNA polymerase by ELISA. * indicated the positive well picked for the next round of screening.

(D and E) Supernatants of single nanobody-expressing clones were detected against *Pfu* DNA polymerase (D) and DR5 (E) by ELISA, respectively. ‡ indicated the single clone isolated for sequencing.

(F) Supernatants of different DR5 nanobody-expressing clones were monitored by ELISA upon dilution with the supernatant of *E. coli* transformed with a naive library of nanobodies by ratios of $1:10^1$, $1:10^2$, $1:10^3$, and $1:10^4$. Data are shown as means ± standard deviations from four independent experiments. **$p < 0.01$ (Student's t tests).

(G and H) Phylogenetic tree showing genetic distances between different nanobodies of *Pfu* DNA polymerase (H) or DR5 (G).

DISCUSSION

Quick isolation of target-specific nanobodies is crucial for both research and therapies. Instead of the widely used screening methods, herein, we developed a method for the discovery of nanobodies from aspects of both theories and practices. Taking advantage of the small molecular weight and the feasibility of nanobodies to be expressed and secreted into the culture media by *E. coli*, our integrated way of screening and expression of specific nanobodies eliminated the step of subcloning of nanobodies into an expression vector. The direct work needed, including cDNA generation (0.5 days), nest PCR (0.5 days), transformation of vectors into *E. coli* (1 day), screening of nanobodies (4–5 days), and production of nanobodies (2 days). The entire work could be done in 8–9 days after the immune response was generated. Thus, this

Table 1. Affinity data for DR5 and *Pfu* with their respective nanobodies

Antigen	Nanobody	K_D [M]
DR5	Nb.Dr01	$(5.4 \pm 0.4) \times 10^{-11}$
	Nb.Dr02	$(9.5 \pm 6.3) \times 10^{-10}$
	Nb.Dr03	$(1.0 \pm 0.1) \times 10^{-7}$
	Nb.Dr04	$(12.0 \pm 1.0) \times 10^{-7}$
	Nb.Dr05	$(1.8 \pm 0.3) \times 10^{-5}$
Pfu DNA polymerase	Nb.Pf01	$(3.5 \pm 0.1) \times 10^{-11}$
	Nb.Pf02	$(3.5 \pm 1.0) \times 10^{-8}$
	Nb.Pf03	$(3.3 \pm 2.1) \times 10^{-5}$
	Nb.Pf04	$(5.9 \pm 2.4) \times 10^{-8}$
	Nb.Pf05	data not available

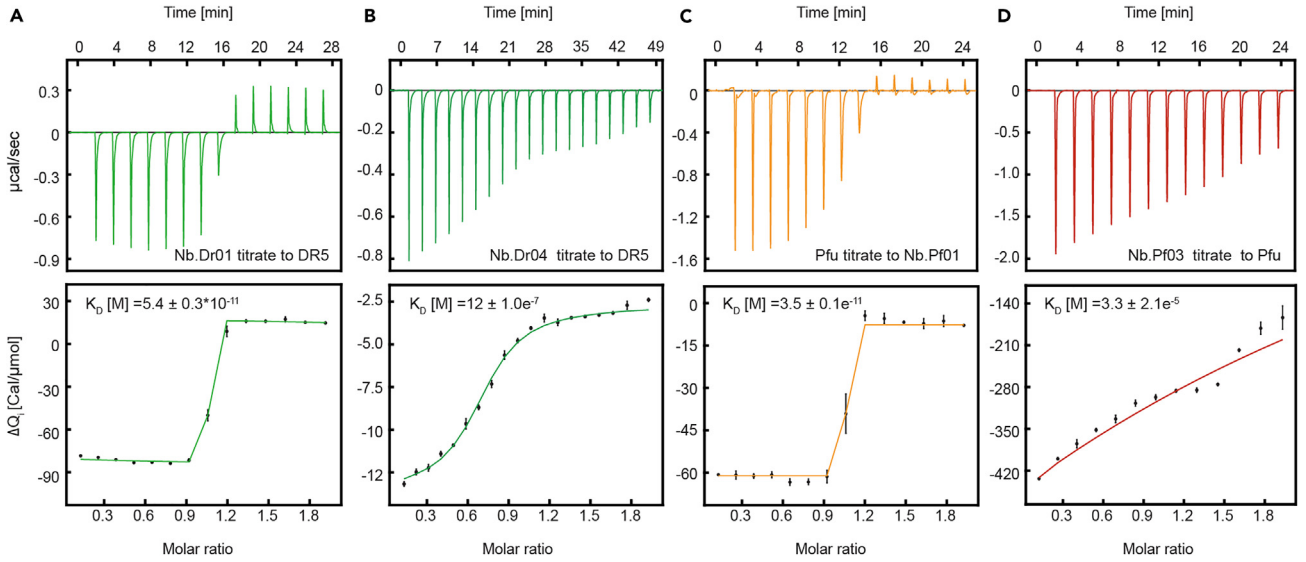

Figure 4. Determination of the binding affinities of isolated nanobodies against their target proteins

(A–D) Representative results from ITC measurements of two monoclonal nanobodies against DR5 protein (A and B) and two monoclonal nanobodies against *Pfu* DNA polymerase (C and D). ITC measurements of all isolated nanobodies against their target proteins are shown in Figure S6.

developed method facilitated reliable, rapid, and integrated screening and production of specific monoclonal nanobodies. Furthermore, this approach allowed nanobody screening at a low cost and worked even without any specialized instruments/devices. In case of limited access to the plate reader, our approach of isolating monoclonal antibodies could still be carried on by identifying positive clones with the naked eye. This is particularly helpful for laboratories in startup companies or labs in developing countries. We demonstrated the highest screening throughput of our method was ~10^6 per 96-well plate. Given the frequency of antigen-specific IgG-secreting B cells often ranged from 10 to 1,000 per 10^6 cells after the immunization,[25] our approach is well suited for the discovery of monoclonal nanobody reagents from the immunized nanobody library. With our modified pET-22b vector, nanobodies are secreted and identified directly from the supernatant of *E. coli* culture media. The isolated target-specific nanobody could be directly used for fermentation to produce nanobodies on a large scale, greatly simplifying the process of production of new nanobodies from scratch.

In comparison with the commonly used phage display method,[16] our approach avoids the problem of artificial loss of library diversity (Table S1). Different phage clones have different growth rates in the common pool of bacteria.[10] During the process of multiple rounds of panning and amplifying of phages, the gene of antibodies carried by the slow-growing phages will be lost.[11] This decrease in library diversity may not be a problem for targets with a single binding site, but it could severely limit the number of useful antibodies identified for targets with different binding epitopes for antibodies. Our approach does not require panning and amplifying of the libraries; therefore, the diversity could be maintained, enabling the identification of as much ligands as possible. Another advantage of our approach is its general applicability: the developed method enables the quick production of a comprehensive repertoire of *Pfu* DNA polymerase and DR5 binding nanobodies. For both DR5 and *Pfu* DNA polymerase, the isolated nanobodies show a wide range of binding affinity from tens of µM to pM, spanning up to 7 orders of magnitude, demonstrating the wide applicability of our methods for isolating nanobodies with a broad range of binding affinities.

In conclusion, our method was shown to enable rapid production of nanobodies with a few rounds of dilution and regrowth of nanobody library-transformed *E. coli* in 96-well plates. The advantages of the integrated screen and expression procedure, low-equipment dependency, and causing no loss of positive clones according to the Poisson distribution convince us our approach has general applicability for nanobody discoveries. Taking into account of advantages of nanobodies, nanobodies can be easily humanized for application in drug development and clinical therapies.[26] They are much smaller than conventional antibodies and could be fused with each other to generate bivalent or multivalent nanobodies.[27] The excellent chemical and thermal stability of nanobodies also promotes their applications in antibody-drug conjugate (ADC) and proteolysis-targeting chimaeras (PROTAC) drugs.[28] We envision that our method for nanobody discovery can be widely implemented in academia and industry to generate nanobody reagents suitable for various applications.

Limitations of the study

Herein, we developed an integrated way of screening and expression of nanobodies, which does not require panning and amplifying of the libraries. The mathematical calculation shows the possibility of the loss of positive clones with our approach is less than 5×10^{-6}, indicating this approach has no bias of the library diversity during the screening process. However, the diversity of the library may be limited by the transformation efficiency of bacteria, which is also a disadvantage encountered by other display technologies[29,30]. Nevertheless, our developed method facilitates rapid simultaneous screening and production of specific monoclonal nanobodies in 8–9 days after the immune response

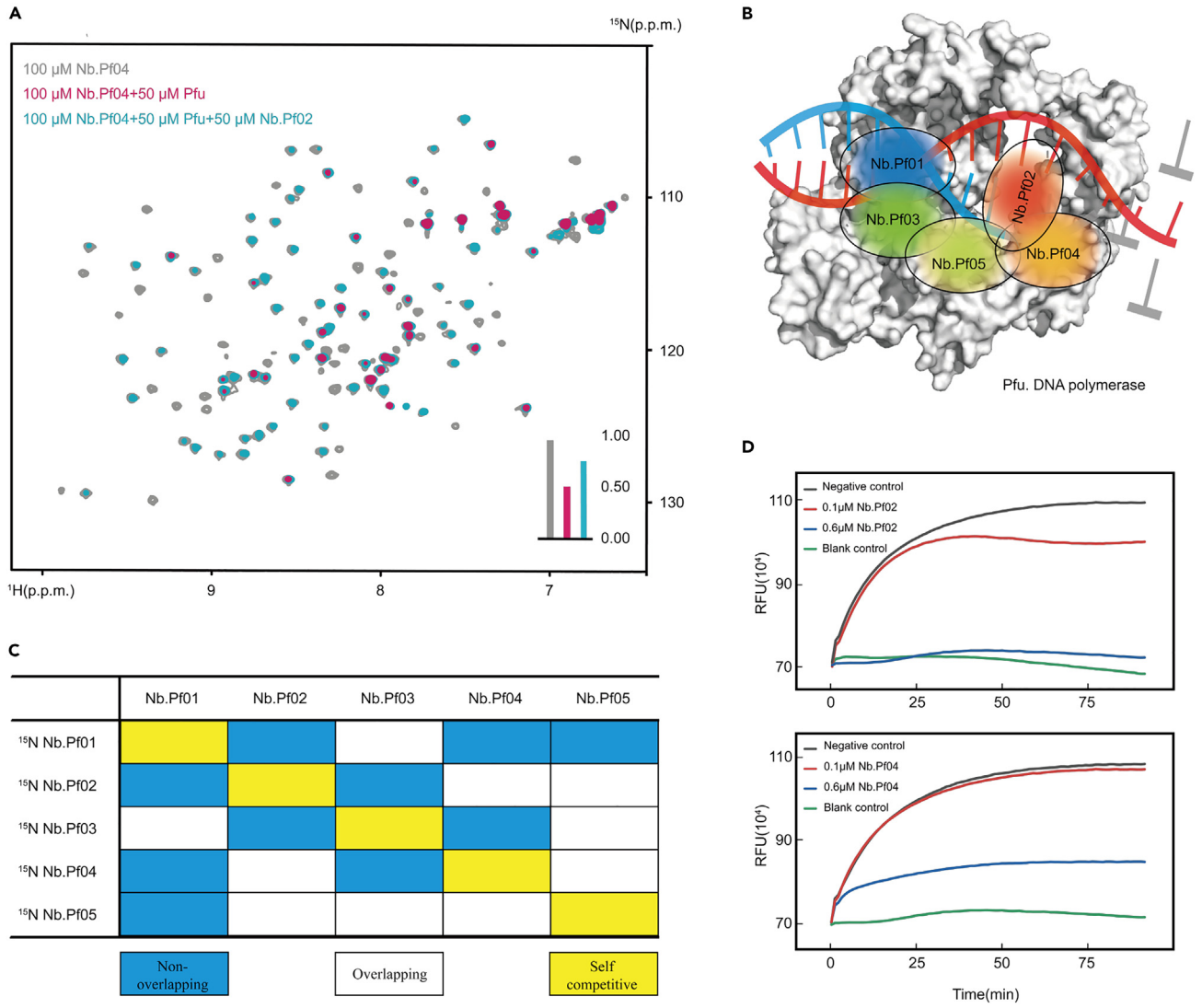

Figure 5. Characterization of the isolated nanobodies against *Pfu* DNA polymerase

(A) ^{15}N-^{1}H HSQC spectra of 100 μM Nb.Pf04 in the presence (magenta) and absence (gray) 50 μM *Pfu* DNA polymerase. Addition of 50 μM unlabeled Nb.Pf02 partially restored the peak intensity of 100 μM Nb.Pf04 with 50 μM *Pfu* DNA polymerase (cyan). All spectra were recorded at 25°C on a Bruker Avance-600 spectrometer. Data were processed in the same way and displayed with the same contour level.

(B) Cartoon representation of binding sites of all five nanobodies on *Pfu* DNA polymerase.

(C) A table summarized the overall competitive status of all five nanobodies upon interacting with *Pfu* DNA polymerase.

(D) The polymerase activity of *Pfu* DNA polymerase was blocked by either Nb.Pf04 or Nb.Pf02 monoclonal nanobody. The green line represented the blank group with no *Pfu* DNA polymerase. The black line represented the control group with *Pfu* DNA polymerase and non-specific nanobody. The red and blue lines represent experimental groups with *Pfu* DNA polymerase and a final concentration of 0.1 μM (red) and 0.6 μM (blue) of the isolated monoclonal nanobody, respectively. Data are represented as mean +/− standard deviations from three independent experiments, **p < 0.01 (Student's t tests).

was generated. Furthermore, this approach allowed nanobody screening at a low cost and worked even without any specialized instruments, showcasing its broad utility potential in the regular generation of monoclonal nanobodies.

STAR★METHODS

Detailed methods are provided in the online version of this paper and include the following:

- KEY RESOURCES TABLE
- RESOURCE AVAILABILITY
  - Lead contact

Table 2. Primers for nested PCR of VHH genes

Primer	Sequence 5′→3′
CALL001	GTCCTGGCTGCTCTTCTACAAGG
CALL002	GGTACGTGCTGTTGAACTGTTCC
VHH-EcoR I-For	CTTGAATTCCATCACCATCACCATCACSAGGTGC AGCTGGTGGAGTCTGGRGGAG
VHH-Hind III-Rev	GGGAAGCTTTTAGCTGGAGACGGTGACCTGGGT

SUPPLEMENTAL INFORMATION

Supplemental information can be found online at https://doi.org/10.1016/j.isci.2024.108966.

ACKNOWLEDGMENTS

This work was supported by National Key R&D Program of China grants 2018YFE0202301 and 2018YFE0202300, National Natural Science Foundation of China grants 22174151 and 21991080, the Strategic Priority Research Program of the Chinese Academy of Sciences XDB0540000, and Hubei Provincial Natural Science Foundation of China 2023AFA041, and Natural Science Foundation of Shandong grants ZR2022MH282.

AUTHOR CONTRIBUTIONS

The research was performed by Z.T., H.W., and X. Zhao; data analysis and validation were performed by Z.T.; manuscript was written by L.H., Z.T., H.W., and X. Zhao; design of the experiments and funds acquirement were conducted by L.H., X. Zhang, J.Z., and M.L. All authors have given approval to the final version of the manuscript.

DECLARATION OF INTERESTS

The authors declare no competing interests.

Received: April 21, 2023
Revised: July 14, 2023
Accepted: January 15, 2024
Published: January 18, 2024

REFERENCES

1. Hamers-Casterman, C., Atarhouch, T., Muyldermans, S., Robinson, G., Hamers, C., Songa, E.B., Bendahman, N., and Hamers, R. (1993). Naturally occurring antibodies devoid of light chains. Nature *363*, 446–448.
2. De Meyer, T., Muyldermans, S., and Depicker, A. (2014). Nanobody-based products as research and diagnostic tools. Trends Biotechnol. *32*, 263–270.
3. Korotkov, K.V., Sandkvist, M., and Hol, W.G.J. (2012). The type II secretion system: biogenesis, molecular architecture and mechanism. Nat. Rev. Microbiol. *10*, 336–351.
4. Toyofuku, M., Nomura, N., and Eberl, L. (2019). Types and origins of bacterial membrane vesicles. Nat. Rev. Microbiol. *17*, 13–24.
5. Gonzalez-Sapienza, G., Rossotti, M.A., and Tabares-da Rosa, S. (2017). Single-Domain Antibodies As Versatile Affinity Reagents for Analytical and Diagnostic Applications. Front. Immunol. *8*, 977.
6. Shin, Y.J., Park, S.K., Jung, Y.J., Kim, Y.N., Kim, K.S., Park, O.K., Kwon, S.H., Jeon, S.H., Trinh, L.A., Fraser, S.E., et al. (2015). Nanobody-targeted E3-ubiquitin ligase

complex degrades nuclear proteins. Sci. Rep. *5*, 14269.
7. Steeland, S., Vandenbroucke, R.E., and Libert, C. (2016). Nanobodies as therapeutics: big opportunities for small anti-bodies. Drug Discov. Today *21*, 1076–1113.
8. Paul, N., Shum, J., and Le, T. (2010). Hot start PCR. Methods Mol. Biol. *630*, 301–318.
9. Valldorf, B., Hinz, S.C., Russo, G., Pekar, L., Mohr, L., Klemm, J., Doerner, A., Krah, S., Hust, M., and Zielonka, S. (2022). Antibody display technologies: selecting the cream of the crop. Biol. Chem. *403*, 455–477.
10. Derda, R., Tang, S.K.Y., Li, S.C., Ng, S., Matochko, W., and Jafari, M.R. (2011). Diversity of phage-displayed libraries of peptides during panning and amplification. Molecules *16*, 1776–1803.
11. Kuzmicheva, G.A., Jayanna, P.K., Sorokulova, I.B., and Petrenko, V.A. (2009). Diversity and censoring of landscape phage libraries. Protein Eng. Des. Sel. *22*, 9–18.
12. Petrenko, V.A., Smith, G.P., Mazooji, M.M., and Quinn, T. (2002). α-helically constrained phage display library. Protein Eng. *15*, 943–950.
13. Yu, X., Orr, C.M., Chan, H.T.C., James, S., Penfold, C.A., Kim, J., Inzhelevskaya, T., Mockridge, C.I., Cox, K.L., Essex, J.W., et al. (2023). Reducing affinity as a strategy to boost immunomodulatory antibody agonism. Nature *614*, 539–547.
14. Ghorashian, S., Kramer, A.M., Onuoha, S., Wright, G., Bartram, J., Richardson, R., Albon, S.J., Casanovas-Company, J., Castro, F., Popova, B., et al. (2019). Enhanced CAR T cell expansion and prolonged persistence in pediatric patients with ALL treated with a low-affinity CD19 CAR. Nat. Med. *25*, 1408–1414.
15. Mao, R., Kong, W., and He, Y. (2022). The affinity of antigen-binding domain on the antitumor efficacy of CAR T cells: Moderate is better. Front. Immunol. *13*, 1032403.
16. Van Campenhout, R., Muyldermans, S., Vinken, M., Devoogdt, N., and De Groof, T.W.M. (2021). Therapeutic Nanobodies Targeting Cell Plasma Membrane Transport Proteins: A High-Risk/High-Gain Endeavor. Biomolecules *11*, 63.
17. Dingus, J.G., Tang, J.C.Y., Amamoto, R., Wallick, G.K., and Cepko, C.L. (2022). A general approach for stabilizing nanobodies for intracellular expression. Elife *11*, e68253.
18. Zhang, Z.X., Nong, F.T., Wang, Y.Z., Yan, C.X., Gu, Y., Song, P., and Sun, X.M. (2022). Strategies for efficient production of recombinant proteins in Escherichia coli: alleviating the host burden and enhancing protein activity. Microb. Cell Fact. *21*, 191.
19. Pal, S., Taylor, H.R., Huneke, R.B., Prendergast, R.A., and Whittum-Hudson, J.A. (1992). Frequency of Antigen-Specific B Cells during Experimental Ocular Chlamydia trachomatis Infection. Infect. Immun. *60*, 5294–5297.
20. Scibelli, A., van der Most, R.G., Turkstra, J.A., Ariaans, M.P., Arkesteijn, G., Hensen, E.J., and Meloen, R.H. (2005). Fast track selection of immunogens for novel vaccines through visualisation of the early onset of the B-cell response. Vaccine *23*, 1900–1909.
21. Parray, H.A., Shukla, S., Samal, S., Shrivastava, T., Ahmed, S., Sharma, C., and Kumar, R. (2020). Hybridoma technology a versatile method for isolation of monoclonal antibodies, its applicability across species, limitations, advancement and future perspectives. Int. Immunopharmacol. *85*, 106639.
22. Shapiro, M.B., Boucher, J., Brousseau, A., Dehkharghani, A., Gabriel, J., Kamat, V., Patil, K., Gao, F., Walker, J., Kelly, R., and Souders, C.A. (2023). Alpaca single B cell interrogation and heavy-chain-only antibody discovery on an optofluidic platform. Antib. Ther. *6*, 211–223.
23. Mitra, S., and Tomar, P.C. (2021). Hybridoma technology; advancements, clinical significance, and future aspects. J. Genet. Eng. Biotechnol. *19*, 159.
24. Madeira, F., Pearce, M., Tivey, A.R.N., Basutkar, P., Lee, J., Edbali, O., Madhusoodanan, N., Kolesnikov, A., and Lopez, R. (2022). Search and sequence analysis tools services from EMBL-EBI in 2022. Nucleic Acids Res. *50*, 276–279.
25. Leyendeckers, H., Odendahl, M., Löhndorf, A., Irsch, J., Spangfort, M., Miltenyi, S., Hunzelmann, N., Assenmacher, M., Radbruch, A., and Schmitz, J. (1999). Correlation analysis between frequencies of circulating antigen-specific IgG-bearing memory B cells and serum titers of antigen-specific IgG. Eur. J. Immunol. *29*, 1406–1417.
26. De Pauw, T., De Mey, L., Debacker, J.M., Raes, G., Van Ginderachter, J.A., De Groof, T.W.M., and Devoogdt, N. (2023). Current status and future expectations of nanobodies in oncology trials. Expert Opin. Investig. Drugs *32*, 705–721.
27. Vincke, C., Loris, R., Saerens, D., Martinez-Rodriguez, S., Muyldermans, S., and Conrath, K. (2009). General strategy to humanize a camelid single-domain antibody and identification of a universal humanized nanobody scaffold. J. Biol. Chem. *284*, 3273–3284.
28. Zhang, H., Han, Y., Yang, Y., Lin, F., Li, K., Kong, L., Liu, H., Dang, Y., Lin, J., and Chen, P.R. (2021). Covalently Engineered Nanobody Chimeras for Targeted Membrane Protein Degradation. J. Am. Chem. Soc. *143*, 16377–16382.
29. Mahdavi, S.Z.B., Oroojalian, F., Eyvazi, S., Hejazi, M., Baradaran, B., Pouladi, N., Tohidkia, M.R., Mokhtarzadeh, A., and Muyldermans, S. (2022). An overview on display systems (phage, bacterial, and yeast display) for production of anticancer antibodies; advantages and disadvantages. Int. J. Biol. Macromol. *208*, 421–442.
30. Marks, J.D. (2004). CHAPTER 32 - Monoclonal Antibodies from Display Libraries. In Molecular Biology of B Cells, T. Honjo, F.W. Alt, and M.S. Neuberger, eds. (Academic Press), pp. 511–531.
31. Conrath, K.E., Lauwereys, M., Galleni, M., Matagne, A., Frère, J.M., Kinne, J., Wyns, L., and Muyldermans, S. (2001). β-Lactamase Inhibitors Derived from Single-Domain Antibody Fragments Elicited in the Camelidae. Antimicrob. Agents Chemother. *45*, 2807–2812.
32. Dumas, P., Ennifar, E., Da Veiga, C., Bec, G., Palau, W., Di Primo, C., Piñeiro, A., Sabin, J., Muñoz, E., and Rial, J. (2016). Extending ITC to Kinetics with kinITC. Methods Enzymol. *567*, 157–180.
33. Pardon, E., Laeremans, T., Triest, S., Rasmussen, S.G.F., Wohlkönig, A., Ruf, A., Muyldermans, S., Hol, W.G.J., Kobilka, B.K., and Steyaert, J. (2014). A general protocol for the generation of Nanobodies for structural biology. Nat. Protoc. *9*, 674–693.
34. Wang, J., Lin, Z., Qiao, C.X., Lv, M., Yu, M., Xiao, H., Wang, Q., Wang, L., Feng, J., Shen, B., et al. (2008). Characterization of a Novel Anti-DR5 Monoclonal Antibody WD1 with the Potential to Induce Tumor Cell Apoptosis. Cell. Mol. Immunol. *5*, 55–60.
35. Kim, S.W., Kim, D.U., Kim, J.K., Kang, L.W., and Cho, H.S. (2008). Crystal structure of Pfu, the high fidelity DNA polymerase from Pyrococcus furiosus. Int. J. Biol. Macromol. *42*, 356–361.

STAR★METHODS

KEY RESOURCES TABLE

REAGENT or RESOURCE	SOURCE	IDENTIFIER
Antibodies		
Mouse Anti-His tag IgG, mAb	GenScript	Cat# A00186; RRID:AB_914704
Goat Anti-mouse IgG [HRP], mAb	Jackson ImmunoResearch Labs (Yeasen Biotech)	Cat# 115-035-003; RRID:AB_10015289
Rabbit Anti-Camelid VHH Antibody [HRP], mAb	GenScript	Cat#A01861; RRID: AB_3083750
Bacterial and virus strains		
T7 Express Competent *E. coli*	NEB	Cat#C2566H
SHuffle® T7 Express Competent *E. coli*	NEB	Cat#C3029J
Biological samples		
Alpaca blood	This paper	N/A
Chemicals, peptides, and recombinant proteins		
SYBR Green I	Yeasen Biotech.	Cat#11171ES03
GERBU adjuvant	GERBU	Cat#3030
Critical commercial assays		
LeukoLOCK™ Total RNA Isolation Kit	Thermo Fisher	Cat#AM1923
TransScript^{R}-Uni One-Step gDNA Removal and cDNA Synthesis	TransGen Biotech Co.	Cat#AU311-02
All-in-One 1st cDNA Synthesis MasterMix kit	Swiss Affinibody LifeScience AG & Qinhe Life Science. Ltd.	Cat#RT001
Deposited data		
Primary Data and uncropped images	This paper	Mendeley Data: doi:10.17632/ynv4mn4k4m.1
Oligonucleotides		
CALL001, CALL002	Conrath et al.[31]	N/A
VHH-EcoR I For and VHH-Hind III-Rev primers	This paper	N/A
Software and algorithms		
AFFINImeter	Philippe et al.[32]	https://www.affinimeter.com
EMBL-EBI	Madeira et al.[24]	https://www.ebi.ac.uk/ebisearch

RESOURCE AVAILABILITY

Lead contact

Further information and requests should be directed to the lead contact, Lichun He (helichun@apm.ac.cn).

Materials availability

This work did not generate new unique reagents.

Data and code availability

Data reported in this paper will be shared by the lead contact upon request.

- This paper does not report original code.
- Original data have been deposited at Mendeley Data and are publicly available as of the date of publication. DOIs are listed in the key resources table.
- Any additional information required to reanalyze the data reported in this paper is available from the lead contact upon request.

EXPERIMENTAL MODEL AND STUDY PARTICIPANT DETAILS

Bacterial strains

The proteins were recombinantly expressed in *E.* coli T7 Express (NEB) or SHuffle T7 Express *E. coli* (NEB). The details of the growth conditions are mentioned in the STAR methods section.

Compliance with ethics requirements

The study was conducted in accordance with the Declaration of Helsinki, and approved by the Laboratory Animal Monitoring Committee of Hubei Province.

METHOD DETAILS

Construction of nanobody immune library

The immunization of llama was performed according to the published protocol.[33] In short, a 3-year-old and a 4-year-old female llama were immunized with six weekly injections of 0.3 mg recombinant DR5 and *Pfu* DNA polymerase respectively, each with equal volumes of GERBU Adjuvant (GERBU Biotechnik GmbH) and recombinant proteins. Both recombinant DR5 and Pfu Polymerase proteins have a purity >95%. 15 mL of peripheral blood was collected after each immunization. 10 mL of peripheral blood was collected as control before the immunization of each llama. Serial dilutions of the pre-immune and immune serum were applied for ELISA to confirm the generation of antigen-specific nanobodies. The blood collected following the final immunization was used for extraction of total RNA with the commercial LeukoLOCK Total RNA Isolation Kit (Thermo Fisher). cDNA was obtained by the reverse transcription of RNA using the All-in-One 1st cDNA Synthesis MasterMix kit (Swiss Affinibody LifeScience AG). The VHH gene segments were amplified by nested PCR using CALL001, CALL002,[31] VHH-EcoRI-For and VHH-HindIII-Rev primers (Table 2) and cloned into a modified pET-22b vector.

Enzyme-linked immunosorbent assays (ELISA)

96-well immune-plates were coated with purified DR5 or *Pfu* DNA polymerase proteins, which were diluted in the coating buffer ($NaHCO_3$-NaOH PH 9.6) at the concentration of 1.0 μg/mL and 10.0 μg/mL for 2 h at 4°C overnight, respectively. 100 μL of supernatants of the nanobody expressing culture media were added to the coated plate for incubation for 2 h at room temperature and then washed 3 times with the PBST (0.5% v/v Tween 20 in PBS PH 7.4) buffer. As the nanobody were all fused with N terminal His tag. A commercial mouse originated anti-His antibody (1: 5000; GenScript) and an anti-mouse IgG-HRP (1: 5000; Yeasen) secondary antibody was applied for the detection of the specifical binding nanobody. The reaction was developed with the colorimetric substrate TMB (3, 3′, 5, 5′-Tetramethylbenzidine) and H_2O_2 for 15 min, followed by the addition of 50 μL 2 M H_2SO_4 to terminate the reaction. The absorption at 450nm was monitored by a microplate reader (Synergy BioTek H1).

Isolation of nanobodies

The integrated screening and expression of nanobodies was named the isolation of nanobodies in our work. Firstly, we did a liquid transformation of the immunized nanobody library into the T7 competent cell to obtain a pool of *E. coli* expressing the immunized nanobody library. The transformation efficiency was determined to be around 10^6 colony-forming units per microgram plasmid. Thus, the volume containing 10^n transformed *E. coli* could be calculated. For the initial screening, a number of 10^n transformed *E. coli* were inoculated in a 96 deep-well plate with 2 mL TB medium and 100 μg/mL Amp in each well. A breath-easy membrane was used to seal the 96 deep-well plate. When OD_{600} reached 0.8, 0.5 mM IPTG was added for induction overnight at 37°C. The plate was then centrifuged at 3000 rpm for 30 min to collect the supernatant. To identify the well containing target-specific nanobodies clones, ELISA was performed as aforementioned. A division of $\lambda \times 10^n$ clones was taken out from the positive well(s), then diluted into 200 mL TB medium and distributed evenly into a second 96 deep-well plate for the next round of target-specific nanobody isolation. The population of positive clone(s) expressing the target-specific nanobody will be enriched by a factor of $\frac{100}{\lambda}$ over each round of isolation according to Poisson distribution. The isolation of target-specific nanobody was repeated till $\lambda \times 10^n \approx 10$. Then, clones from the positive well were spread on the LB agar plate with 100 μg/mL Amp to get separated single clones of *E. coli*. Single clones were then inoculated into a new 96 deep-well plate with one clone in each well for the final round of isolation to get the target-specific monoclonal nanobodies. A value of n in between 1 and 3 was recommended for the initial isolation step dependent on the abundance of the target-specific IgG secreting B cells in the peripheral blood. λ value of 10 was used in this work.

Isothermal titration calorimetry (ITC)

DR5, *Pfu* DNA polymerase and nanobodies were expressed and purified according to the published protocols.[34,35] Protein samples were dialyzed to the same buffer (20mM HEPES-NaOH、150 mM NaCl pH 8.0) at 4°C overnight prior to experiments. Protein concentrations were determined after dialysis. ITC Experiments were performed using the Malvern MicroCal PEAQ-ITC system with 10–50 μM antigen proteins or nanobodies in the reaction cell and 100 to 500 μM of the interacting nanobodies and antigen proteins in the injection syringe. Experiments were performed under stirring at 750 r.p.m. at 25°C. The initial injection was 0.4 μL, following by a series of injections of 2.5 μL. Data was analyzed with the AFFINImeter[32] software.

Nuclear Magnetic Resonance (NMR) spectroscopy

Pfu DNA polymerase and its corresponding monoclonal nanobodies were dialyzed in the sodium phosphate buffer (20 mM sodium phosphate,150 mM NaCl pH 7.4) at 4°C overnight. 100 μM of ^{15}N-labeled nanobody with 5% of D_2O were applied for 2D [^{15}N,^{1}H]-HSQC measurement in the absence and presence of 50 μM *Pfu* DNA polymerase. 50 μM of a mutually different unlabeled nanobody was then added in the NMR sample of ^{15}N-labeled nanobody with 50 μM *Pfu* DNA polymerase to identify if two nanobodies shared overlapping binding sites on the *Pfu* DNA polymerase. All NMR spectra were measured at 298 K on a Bruker Avance-600 MHz spectrometer equipped with a TCI cryoprobe. Data were processed with the Topspin software and displayed with the same contour level.

Pfu DNA polymerase activity blocking assay

Real-Time Quantitative PCR was applied to verify the blocking effect of the isolated nanobodies on the activity of the *Pfu* DNA polymerase. A single-stranded DNA incubation experiment was performed with 1U *Pfu* DNA polymerase, 200 μM dNTP, 20 mM Tris-HCl, 10 mM KCl, 0.1% Triton X-100, 0.1 mg/mL BSA, 2 mM $MgSO_4$, 10 mM $(NH_4)_2SO_4$, 1X of SYBR Green I, pH 8.8. The experiment group was performed with the addition of 0.1 μM or 0.6 μM isolated *Pfu* monoclonal nanobody. The negative control group was carried on with the addition of 0.6 μM non-specific nanobody. Another blank control was performed without *Pfu* DNA polymerase. The experimental procedure was 50°C 1 min, 90 cycles. All experiments were run in triplicate.

QUANTIFICATION AND STATISTICAL ANALYSIS

All qPCR experiments were conducted in biological triplicates, error bars represent mean standard error mean and analyzed using the Origin Pro 2019 software. Student's t-tests were employed to designate the statistical significance and $p < 0.05$ considered significant. ITC data was analyzed with the AFFINImeter software. NMR data were processed with the Topspin software.

ADDITIONAL RESOURCES

Primary Data and uncropped images can be found online at Mendeley Data. doi:10.17632/ynv4mn4k4m.2.